

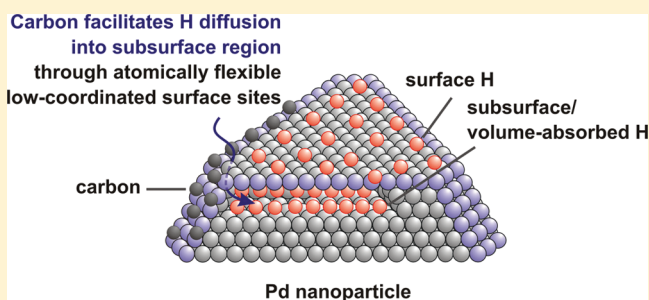
Subsurface Hydrogen Diffusion into Pd Nanoparticles: Role of Low-Coordinated Surface Sites and Facilitation by Carbon

Wiebke Ludwig,[†] Aditya Savara,[†] Robert J. Madix,[‡] Svetlana Schauermaⁿ,^{*,†} and Hans-Joachim Freund[†]

[†]Fritz-Haber-Institut der Max-Planck-Gesellschaft, Faradayweg 4-6, 14195 Berlin

[‡]School of Engineering and Applied Science, Harvard University, G-14 Pierce Hall, 29 Oxford Street, Cambridge, Massachusetts 02138, United States

ABSTRACT: Hydrogen species absorbed in the volume of Pd nanoparticles play a crucial role in the hydrogenation of unsaturated hydrocarbons. Recent evidence suggests that the rate of diffusion of hydrogen from the surface of Pd nanoparticles to the subsurface region critically affects the hydrogenation rate, as this rate dictates whether or not the nanoparticles can maintain a sufficient concentration of subsurface hydrogen species under operating conditions. Recent theoretical calculations predicted pronounced facilitation of subsurface hydrogen diffusion by coadsorbed carbon and identified the conceptual importance of atomically flexible low-coordinated surface sites on small metal clusters for the diffusion process. In this study, we experimentally probe the kinetics of hydrogen diffusion into the subsurface by performing pulsed molecular beam experiments on carbon-free and carbon-containing Pd nanoparticles and on Pd(111). We provide experimental proof that low-coordinated surface sites on Pd particles play a crucial role in the diffusion process and that their selective modification with carbon results in marked facilitation of subsurface hydrogen diffusion, in line with the theoretical predictions.



1. INTRODUCTION

The ability of nanoscale transition metal clusters to absorb atomic hydrogen has pivotal importance for a large variety of industrially relevant applications, such as hydrogen storage and purification materials, development of fuel cells, and switchable mirrors.^{1,2} In heterogeneous catalysis, the crucial role of hydrogen absorbed in the subsurface region of the active metal phase was recently established in a number of surface science studies on hydrogenation of alkenes and alkynes.³⁻⁶ For these applications, activated hydrogen diffusion into the subsurface of a metal particle is an essential elementary step, which can critically control the overall performance of the catalyst.^{6,7} Recent mechanistic studies on olefin hydrogenation provided evidence that sustained catalytic activity on Pd nanoparticles is only achieved when the subsurface hydrogen reservoir can be effectively replenished under reaction conditions,^{6,7} and it was proposed that this replenishment process can only efficiently proceed in the presence of carbon.^{6,7} Although the important role of carbonaceous deposits in the activity and selectivity of transition metals has been recognized for a long time in the catalytic community,⁸ a microscopic understanding of how carbon participates in surface processes which involve hydrogen is largely missing. Traditionally, carbon is considered to merely play the role of a site-blocker in surface processes on metals. However, recent microscopic insights into hydrocarbon surface chemistry and hydrogen-related processes do not support this common way of discussing the role of carbonaceous deposits⁵⁻⁷ and kindle the

need for additional microscopic concepts to describe the fundamentals of hydrogenation catalysis.

The interaction of hydrogen with transition metals was extensively studied by both experimental and theoretical methods for several decades,⁹⁻¹² yet the microscopic details of the hydrogen subsurface diffusion process remain largely unexplored. This is mainly because the range of experimental tools which are sensitive to hydrogen and which are capable of addressing the dynamics of hydrogen diffusion in a time-resolved way is very limited. Theoretical calculations on hydrogen diffusion into the subsurface region of Pd clusters revealed the conceptual importance of the atomic flexibility of metal nanoparticles.¹³ In these calculations, lateral atomic flexibility of small Pd clusters enabled the expansion of the lattice near the particle edges during the diffusion event. This effect was calculated to result in a substantial reduction of the activation barrier for hydrogen diffusion into the subsurface and thus substantial facilitation of the hydrogen diffusion rate into Pd clusters relative to an atomically stiff extended Pd(111) face. The computations indicate that a significant expansion of the lattice near the particle edges can be achieved by modification of the low-coordinated sites with carbon, which is predicted to nearly remove the barrier for diffusion of hydrogen into the subsurface. These effects were envisaged to have a decisive

Received: September 19, 2011

Revised: December 5, 2011

Published: January 3, 2012

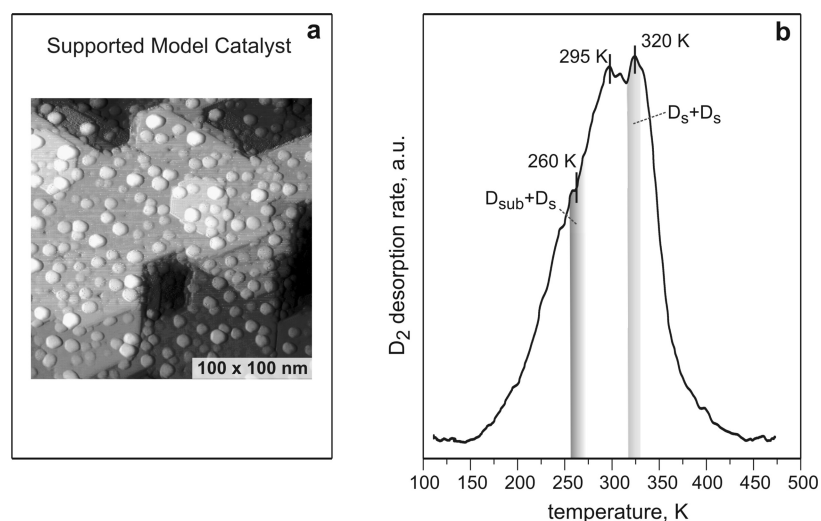


Figure 1. (a) Scanning tunnelling microscopy (STM) image (100 nm \times 100 nm) of the Pd/Fe₃O₄/Pt(111) supported model catalyst used in the experiments described here (from ref 14). (b) TPD spectrum obtained after adsorption of 3.1 L of D₂ on the Pd/Fe₃O₄/Pt(111) model catalyst at 100 K.

influence on catalytic processes such as hydrogenation, which depend on the effective replenishment of subsurface hydrogen. In line with this suggestion, it was recently observed experimentally that modification of the low-coordinated surface sites of Pd nanoparticles, such as edges and corners, with carbon results in a sustained hydrogenation rate of 2-butene that is not possible on the C-free surface.^{6,7} This observation was proposed to arise from faster subsurface diffusion of hydrogen through the edge sites modified with carbonaceous deposits.

In this study, we for the first time experimentally address the kinetics of hydrogen diffusion into the subsurface on well-defined model Pd nanoparticles and on Pd(111) by performing pulsed multimolecular beam experiments. Particular emphasis was placed on understanding the role of atomically flexible low-coordinated surface sites, such as the edges and corners, in the diffusion process and on exploring how modification of these surface sites with carbon affects the subsurface diffusion rate. To probe hydrogen subsurface diffusion, the H₂ + D₂ \rightarrow HD exchange reaction was conducted in the temperature regime where the rate of this reaction is limited by the formation rate of the subsurface H(D) species. We provide direct experimental evidence that—in line with theoretical predictions—the atomically flexible low-coordinated surface sites on Pd particles play a crucial role in the diffusion process and that selective modification of these sites with carbon results in marked facilitation of subsurface hydrogen diffusion. The latter finding allows us to identify adsorbed carbon as an exceptionally important participant in surface reactions, which governs the rate of subsurface hydrogen diffusion, and to revisit the traditional view on the role of carbonaceous deposits in hydrogenation chemistry.

2. RESULTS AND DISCUSSION

The model catalyst used in this study is shown in Figure 1a. It consists of Pd nanoparticles of \sim 7 nm size (Figure 1a) supported on a well-ordered Fe₃O₄/Pt(111) thin film. The particles are mainly terminated by (111) facets (\sim 80% of the surface area) and exhibit low-coordinated surface Pd atoms incorporated into edges, corners, and (100) facets.¹⁴ Sub-monolayer amounts of carbon were deposited by adsorption of

cis-2-butene and D₂ followed by heating to 485 K (for experimental details and the carbon deposition procedure see the Experimental Section). The spatial distribution of the carbonaceous deposits was previously investigated by IR spectroscopy using CO as a probe molecule for different adsorption sites. It was established that the carbon occupies predominately edge sites of the Pd nanoparticles while leaving the regular (111) terraces nearly unchanged.¹⁵

Hydrogen ad- and absorption on model supported Pd nanoparticles was previously extensively characterized both by temperature programmed desorption (TPD)^{4,15,16} and by hydrogen depth profiling via nuclear reaction analysis (NRA).¹⁶ Figure 1b shows a desorption trace of D₂ from Pd particles obtained after adsorption of 3.1 L of D₂ at 100 K. Two distinct peaks with maxima at 295 and 320 K can be identified. By performing hydrogen depth profiling via NRA, it was possible to clearly attribute the high-temperature peak to associative recombination of strongly bound H(D) species adsorbed on the surface. The estimated desorption energy of 83 kJ·mol⁻¹ is very similar to the value 87 kJ·mol⁻¹ measured for hydrogen desorption from Pd(111) in the low-coverage limit, where only strongly bound surface species are populated.¹⁷ The desorption of H₂(D₂) in the low-temperature regime (between 200 and \sim 300 K) was found to be associated with the depletion of weakly bound H(D) species *absorbed* in the bulk of Pd particles.¹⁶ It should be emphasized that in this low-temperature regime only the depletion of subsurface species was observed upon heating by NRA, while the concentration of surface H(D) was observed to remain constant, implying that the low-temperature desorption pathway involves consumption of at least one subsurface H species. It is likely that a surface-adsorbed H atom is also involved in this pathway as a participant. In this case, a desorption event must be accompanied by a simultaneous replenishment of the surface H(D) reservoir from the H-containing volume of Pd particles.

The clear distinction of two desorption regimes allowed us to separately probe the processes dominated by associative desorption of subsurface or subsurface-related species (indicated here as D_{sub} or H_{sub}) versus processes governed mainly by desorption of the more strongly bound surface species (D_s or H_s). For this purpose, the following experimental approach

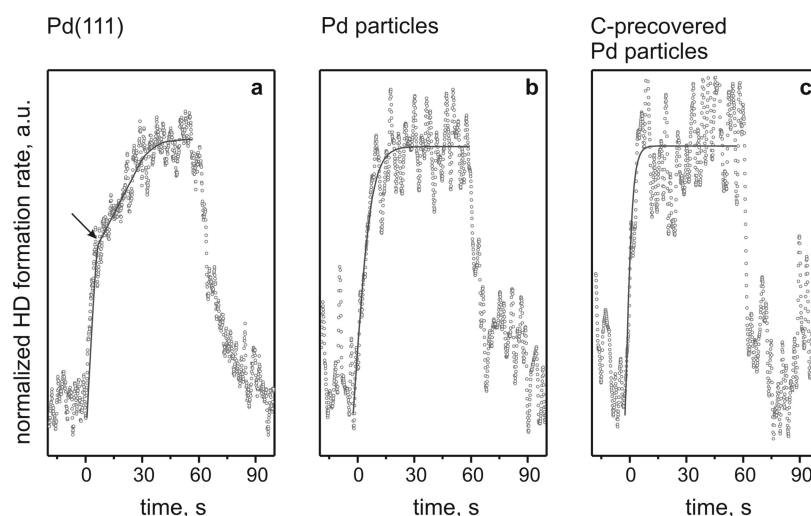


Figure 2. Time evolution of the HD formation rate obtained at 280 K on (a) Pd(111), (b) pristine Pd nanoparticles supported on $\text{Fe}_3\text{O}_4/\text{Pt}(111)$, and (c) C-precovered Pd nanoparticles. The sample was exposed to a continuous D_2 beam and to a pulsed H_2 beam. The H_2 exposure pulse starts at time zero and ends at 60 s. Each plot of data above was obtained by averaging pulse profiles from three independent measurements. The arrow indicates the inflection point (see text).

was used: we exposed the model catalyst to a continuous D_2 molecular beam with a flux of 3.2×10^{15} molecules $\cdot\text{cm}^{-2}\cdot\text{s}^{-1}$, until both the surface and the volume of the Pd particles were saturated with D, and then applied 60 s long pulses of H_2 from a second molecular beam (flux: 4.5×10^{13} molecules $\cdot\text{cm}^{-2}\cdot\text{s}^{-1}$), thereby generating a reactant ratio of $\text{D}_2:\text{H}_2 = 71$ impinging upon the surface. Note that the absolute flux of H_2 is small compared to that of D_2 (less than 1.5%), which ensures that the steady state concentrations of the D species are not perturbed by the reaction with H species.

The time evolution of the reaction product, HD, was monitored by quadrupole mass spectrometry (QMS). At a sufficiently low reaction temperature (260–280 K), the HD formation rate, which is equivalent to the desorption rate, is dominated by association of subsurface-related species (note that at these temperatures the dominant pathway results in consumption of subsurface species but does not necessarily occur via recombination of two subsurface species). Consistent with this interpretation, the mean residence time of the surface hydrogen species is estimated to be ~ 3000 s at 260 K in the absence of subsurface hydrogen,¹⁸ which is approximately 2 orders of magnitude larger than H_2 pulse duration of these experiments. In conjunction with the NRA data, this estimate of the mean residence time strongly suggests that the rate of HD formation at <280 K is dominated by reactions involving the subsurface or subsurface-related $\text{H}_{\text{sub}}(\text{D}_{\text{sub}})$ species and that the contribution to the HD production rate from reactions between surface atoms is negligible. In contrast, at a reaction temperature of 320 K, the subsurface $\text{H}_{\text{sub}}(\text{D}_{\text{sub}})$ reservoir would be essentially depleted, and the HD formation would occur mainly via recombination of the more strongly bound surface H_s and D_s .

Figure 2 shows the time evolution of the HD formation rate in response to the H_2 beam pulse in the low-temperature regime for three surfaces: Pd(111) and clean and C-precovered Pd nanoparticles. On Pd(111) (Figure 2a), a clear parallel reaction behavior can be observed: after the H_2 beam is opened, the rate of HD formation increases rapidly at first and then exhibits an inflection point before reaching a steady state value after ~ 40 s. The height of the final plateau is about twice that of

the inflection point. On clean and C-precovered Pd particles, a similar fast increase of the reaction rate is observed initially—up to the inflection point—but the second increase to a steady state level occurs more rapidly—in about 9 s for the C-free and 6 s for the C-precovered Pd particles.

The initial fast-rising component of the HD formation rate can be rationalized as HD formed from reaction between D_{sub} (which is already present in the particles) and surface H_s , formed by spontaneous nonactivated dissociation of H_2 on Pd surface. Such fast and nonactivated dissociation is typical for Pd and a number of other transition metal surfaces.¹¹ In contrast, the slower component of the HD rate can originate from reaction between D_s and H_{sub} , the latter species being formed in a slower activated process of H diffusion into the subsurface.¹¹ Within the scope of this model, the reaction rate R_{HD} of the low-temperature channel can be expressed as

$$R_{\text{HD}}(t) = k_{\text{sub}}[\text{D}_{\text{sub}}][\text{H}_s(t)] + k_{\text{sub}}[\text{D}_s][\text{H}_{\text{sub}}(t)] \quad (1)$$

where k_{sub} is the reaction rate constant for the low-temperature pathway; $[\text{D}_s]$ and $[\text{D}_{\text{sub}}]$ are the steady state concentrations of the surface and subsurface-related D species; and $[\text{H}_s(t)]$ and $[\text{H}_{\text{sub}}(t)]$ are the time-dependent concentrations of the surface and subsurface-related H species. Note that after establishing the steady state conditions the ratios $[\text{D}_s]:[\text{H}_s] = [\text{D}_{\text{sub}}]:[\text{H}_{\text{sub}}] = 71$ (equal to the ratio of the reactants in the gas phase) and the contributions of both terms in eq 1 should be equal, i.e., $k_{\text{sub}}[\text{D}_{\text{sub}}][\text{H}_s] = k_{\text{sub}}[\text{D}_s][\text{H}_{\text{sub}}] = (1/71)k_{\text{sub}}[\text{D}_{\text{sub}}][\text{D}_s]$.¹⁹ This condition is reasonably fulfilled for Pd(111), where the contributions of both parts of the composite curve can be most easily estimated (Figure 3). It should be pointed out that the observed parallel reaction behavior at this temperature and at constant D coverage suggests a reaction mechanism involving the direct association of the subsurface D(H) with the surface-adsorbed H(D) species, particularly in view of the previous NRA results. If only one type of surface species (i.e., the surface species with modified adsorption properties by the presence of subsurface H(D)) was involved in HD formation, only a single reaction channel could occur.

The initial rate of H_{sub} accumulation directly depends on the rate constant for subsurface hydrogen diffusion

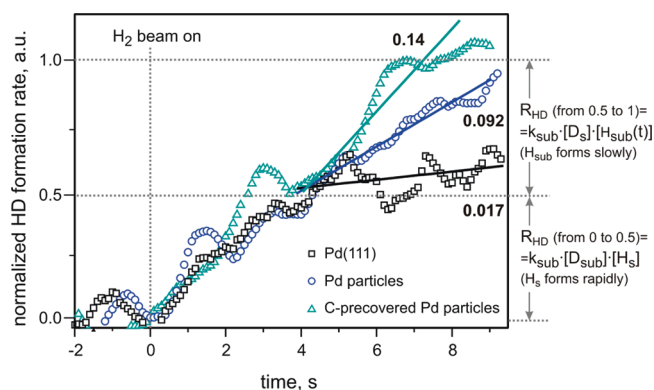


Figure 3. Comparison of the pulse profiles of the normalized HD formation rate for Pd(111) and pristine and C-covered Pd nanoparticles using the same data shown in Figure 2. The time evolution of the normalized HD formation rate coincides for all surfaces until the rate reaches the value 0.5 and then diverges significantly afterward.

$$\frac{d\theta_{\text{H}_{\text{sub}}}(t)}{dt} = k_{\text{diff}}[\text{H}_{\text{s}}(t) - \text{H}_{\text{sub}}(t)] - k_{\text{sub}}[\text{D}_{\text{s}}][\text{H}_{\text{sub}}(t)] \quad (2)$$

where k_{diff} is the rate constant for diffusion into the subsurface. In this formulation, the diffusion rate is assumed to be proportional to the difference between the concentration of H_{s} and H_{sub} .

Once the steady state concentration of H_{s} is rapidly reached (the fast rise in the HD production), the *initial* formation rate of H_{sub} is given by $((d\theta_{\text{H}_{\text{sub}}}(t=0))/(dt)) \approx k_{\text{diff}}[\text{H}_{\text{s}}]$. Thus, the observed slower rise of the second component of the reaction process to the steady state on the close-packed Pd(111) relative to the Pd particles indicates a slower rate of formation of H_{sub} on the extended Pd(111) single crystal than on the Pd particles. We interpret the data to mean that in all cases the surface species H_{s} quickly reaches the steady state concentration expected for both Pd(111) and Pd(100) faces in this temperature range, while the slower formation rate of H_{sub} on Pd(111) relative to the Pd particles is attributable to the lower k_{diff} . Faster formation of H_{sub} on Pd particles may be due to the atomic flexibility of the nanoclusters, particularly at low-coordinated surface sites, such as edges and corners, which should allow for easier H penetration into the volume of the particles. This experimental result is also in agreement with the previous experimental observations that lower exposures of H_2 are needed to populate the subsurface species on the open (100) and (110) surfaces as compared to the close-packed (111) face.^{11,20,21}

The time evolution of the two parallel reactions that contribute to the overall HD formation rate can be most easily compared by normalizing the reaction rates to their steady state values. Figure 3 shows normalized HD formation rates for the first 10 s of the H_2 pulses on Pd(111) and on both clean and C-precovered Pd particles. All three curves overlap until HD production reaches half of the steady state value after ~ 4 s of H_2 exposure ($R_{\text{HD}(\text{from } 0 \text{ to } 0.5)}$) and then diverges significantly thereafter ($R_{\text{HD}(\text{from } 0.5 \text{ to } 1.0)}$). The coincidence of the rate profiles at the beginning of the H_2 pulse is in excellent agreement with the reaction mechanism proposed above, which suggests that one-half of the final steady state reaction rate ($R_{\text{HD}(\text{from } 0 \text{ to } 0.5)} = k_{\text{sub}}[\text{D}_{\text{sub}}][\text{H}_{\text{s}}]$) arises from the reaction of

D_{sub} , already available in the particles, with the quickly forming H_{s} species. Additionally, the characteristic time for the formation of surface-adsorbed H_{s} is surface-independent for the three surfaces in Figure 3 (at least on the time scale of observation), which agrees well with the fast nonactivated formation of surface H_{s} species described in the literature for most of the transition metal surfaces including Pd.¹¹

In contrast, for the time evolution of the second half of the reaction rate ($R_{\text{HD}(\text{from } 0.5 \text{ to } 1.0)} = k_{\text{sub}}[\text{D}_{\text{s}}][\text{H}_{\text{sub}}(t)]$), a strong dependence on the surface structure is observed, which we attribute to the slow structure-dependent subsurface H diffusion. This dependence can be quantified in terms of the slope of the curve directly after the level of HD production reaches *half* that of the maximum steady state value ($R_{\text{HD}} = 0.5$, see the linear fit in Figure 3). In view of the fact that at this reaction temperature the surface state is saturated both on Pd(111) and Pd particles with a coverage of about 1, and given that $(\text{H}_{\text{s}} - \text{H}_{\text{sub}}) \sim \text{H}_{\text{s}}$, the differences in the slopes reflect the differences in the values for k_{diff} for the Pd(111) surface and the Pd nanoparticles. Note that based on this slope the rate constant for diffusion of H into the subsurface is nearly an order of magnitude higher on the C-covered Pd particles compared to the close-packed Pd(111) surface. Taking into account the small relative fraction of the low-coordinated surface sites on the Pd particles ($\sim 20\%$), the rate constant for H diffusion through the C-modified edge sites of the Pd particles is estimated to be at least a factor of 50 greater than that for diffusion through the Pd(111) face. Note that the contributions from the two rate terms in eq 1, which correspond to the two possible HD formation channels, are predicted to be equal. The observed experimental data are in an excellent agreement with this prediction as indicated by the fact that the reaction rate obtained after the first four seconds (the maximum reaction rate of the “fast channel”) is exactly half of the final steady state HD formation rate.

In terms of the model, the reaction rate at 320 K can be expressed as

$$R_{\text{HD}}(t) = k_{\text{s}}[\text{D}_{\text{s}}][\text{H}_{\text{s}}(t)] + k_{\text{sub}}[\text{D}_{\text{sub}}][\text{H}_{\text{s}}(t)] + k_{\text{sub}}[\text{D}_{\text{s}}][\text{H}_{\text{sub}}(t)] \quad (3)$$

where k_{s} is the reaction rate constant for the high-temperature pathway.

As discussed earlier, at 320 K the contribution from the reaction between pairs of strongly adsorbed surface species (not modified by the presence of subsurface hydrogen) H_{s} and D_{s} (first term in eq 3) most likely dominates the overall reaction rate. This is because the concentrations of the subsurface species (H_{sub} and D_{sub}) are very small at 320 K, according to both the NRA and TPD results, and therefore the reaction channel associated with the subsurface species becomes minor. Assuming fast formation of the surface-adsorbed H_{s} species, the model predicts a transition from the time-dependent sigmoidal behavior of the product pulses (in Figure 3) to a more rectangular pulse form. Indeed, a nearly perfect square-shaped HD production profile was observed on both Pd(111) and Pd nanoparticles (Figure 4). Thus, the suggested mechanistic model correctly accounts for the temperature dependence of the HD formation rate at both low temperatures and high temperatures. It should be noted that while virtually no subsurface hydrogen is present at 320 K under the low-pressure conditions applied in this study substantial amounts of hydrogen incorporated into Pd bulk are expected to be present

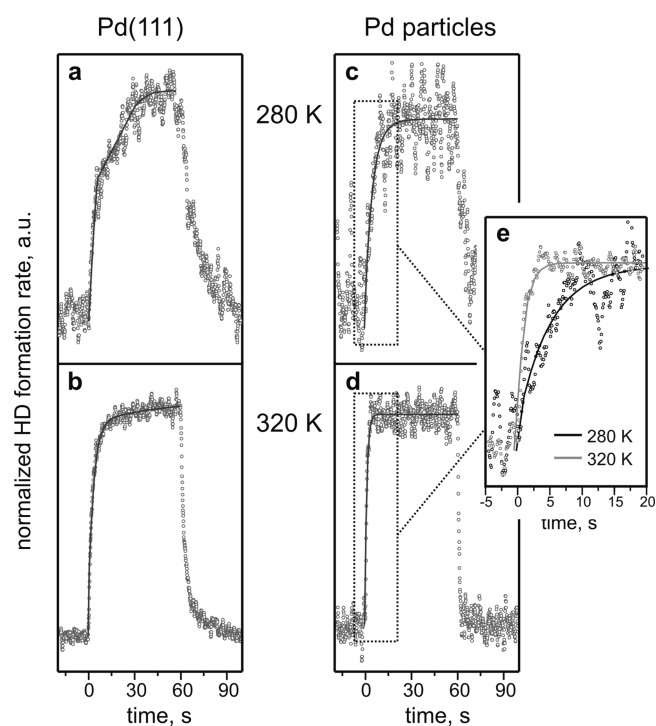


Figure 4. Time evolution of the HD formation rate obtained using Pd(111) at (a) 280 K and (b) 320 K and using pristine Pd nanoparticles supported on $\text{Fe}_3\text{O}_4/\text{Pt}(111)$ at (c) 280 K and (d) 320 K. (e) Comparison of the pulsed profiles obtained at 280 and 320 K on the pristine Pd nanoparticles. Data were obtained as described for Figure 2. In agreement with the suggested kinetic model, increasing the temperature from 280 to 320 K results in a transition from a clear bimodal behavior at 280 K to a nearly rectangular-shaped pulse profile at 320 K for the HD formation rate.

under normal industrial pressure conditions, even in the temperature range of 300–500 K (see, e.g., the H–Pd phase diagrams in refs 22 and 23). This means that the reaction mechanisms involving subsurface hydrogen can apply in a broad range of practically relevant temperatures and pressures.

Finally, we address how carbon deposition at the low-coordinated sites of Pd nanoparticles affects the diffusion process. We probed the HD exchange in a range of pressure conditions from 1.3×10^{-6} to 5.3×10^{-6} mbar (overall pressure), keeping the reactant ratio constant at $\text{D}_2:\text{H}_2 = 71$. Figure 5 shows the steady state HD formation rates obtained in these experiments for the reaction temperatures 260 and 320 K. Carbon was found to affect the HD formation rate in a dramatically different way for the two reaction temperatures: whereas at 320 K preadsorbed carbon *reduces* the overall reaction rate by about 30%, the reaction rate *increases* by about 100% at 260 K on the carbon-precovered particles, for all pressures studied. The decreased HD formation rate in the high-temperature regime, where HD formation is most likely dominated by the recombination of the surface-adsorbed species, can be easily rationalized as a consequence of the blocking of adsorption sites by carbon. Interestingly, despite the fact that a part of the surface is blocked by carbon, the HD formation rate significantly increases in the low-temperature regime: where desorption is dominated by recombination of the subsurface-related species. This effect can be explained by the higher formation rate of the subsurface H(D) species on the C-modified particles resulting in a higher steady state concentration of these species in the subsurface. This result is

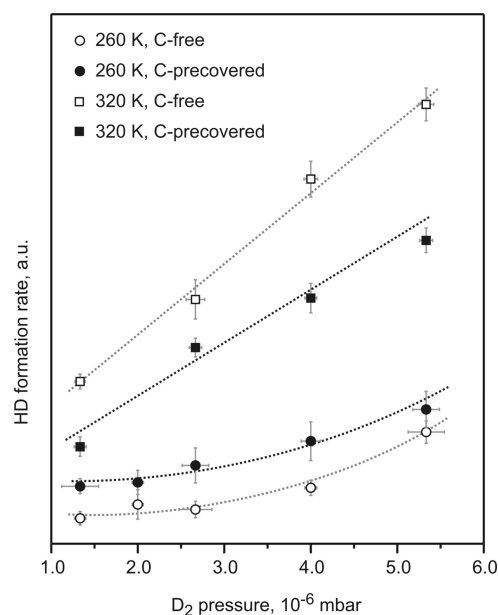


Figure 5. Steady state HD formation rates obtained on the pristine and C-precovered Pd nanoparticles supported on $\text{Fe}_3\text{O}_4/\text{Pt}(111)$ at 260 and 320 K in the D_2 pressure range from 1.3×10^{-6} to 5.3×10^{-6} mbar. The reactant ratio $\text{D}_2:\text{H}_2$ was kept constant at 71. Carbon deposition resulted in a $\sim 30\%$ decrease in the HD formation rate at 320 K and in a $\sim 100\%$ increase in the HD formation rate at 260 K.

in perfect agreement with the time evolution of the HD product presented in Figures 2 and 3, which also suggests that the effective subsurface diffusion rate constant (k_{diff}) on the Pd particles increases after C deposition by about a factor of 2. It should be noted that at the microscopic level facilitation of subsurface H diffusion through the C-modified low-coordinated sites is most likely even more pronounced than this factor of 2. Indeed, the nearly 100% increase of the overall subsurface diffusion rate arises from modification of only $\sim 20\%$ of the surface sites constituting edges and corners of Pd particles. Microscopically, this means that the *local* diffusion rate through these C-modified sites increases by at least an order of magnitude. These results are in excellent qualitative and in a good quantitative agreement with the theoretical predictions.¹³

3. CONCLUSIONS

In conclusion, we have probed the kinetics of diffusion of hydrogen into Pd nanoparticles using pulsed multimolecular beam experiments and HD production as an indicator of the presence of subsurface hydrogen. The HD exchange reaction was carried out in a temperature regime where its rate is limited by the rate of formation of subsurface H species and under conditions where the process of subsurface H diffusion occurs at experimentally measurable time scales. By comparing the time evolution of the HD product using the model supported Pd nanoparticles and the extended Pd(111) surface, we show that the H subsurface diffusion critically depends on the structure of the surface and is considerably facilitated on the atomically flexible Pd nanoparticles. Moreover, in agreement with theoretical predictions, modification of the atomically flexible low-coordinated surface sites, such as edges and corners, with carbon was found to increase the subsurface diffusion rate by at least an order of magnitude. These findings clarify the microscopic origin of the previously experimentally observed promotion of *sustained* hydrogenation activity on the

C-modified Pd nanoparticles, which requires effective replenishment of the subsurface hydrogen species. The observed phenomena provide important insights into the microscopic details of hydrogen interaction with technically relevant transition metal surfaces and underline the exceptional importance of the atomic flexibility of metal nanoparticles and surface modifiers such as carbon that is usually formed under catalytic reaction conditions. Related effects are expected to play a key role in processes taking place on a large variety of hydrogen storage and catalytic materials.

4. EXPERIMENTAL SECTION

All molecular beam (MB) experiments were performed at the Fritz-Haber-Institut (Berlin) in a UHV apparatus described in detail previously.²⁴ Two effusive doubly differentially pumped multichannel array sources operated at room temperature were used to supply the D₂ and H₂. Beam fluxes for D₂ between 1.0×10^{15} and 4.3×10^{15} molecules·cm⁻²·s⁻¹ (1.3×10^{-6} to 5.3×10^{-6} mbar on the sample surface) and for H₂ between 1.5×10^{13} and 6.0×10^{13} molecules·cm⁻²·s⁻¹ (1.5×10^{-8} to 5.3×10^{-8} mbar) were used in these experiments. An automated quadrupole mass spectrometer (QMS) system (ABB Extrel) continuously monitored the partial pressure of the reactants (H₂ at 2 amu and D₂ at 4.8 amu) and products (HD at 3 amu).

The Pd/Fe₃O₄ model catalyst was prepared by growing a thin (~100 Å) Fe₃O₄ film on a Pt(111) single crystal by repeated cycles of Fe (>99.99%, Goodfellow) physical vapor deposition and subsequent oxidation (see refs 14 and 25 for details). The cleanliness and quality of the oxide film was checked by IRAS of adsorbed CO and by LEED. Pd particles (>99.9%, Goodfellow) were grown by physical vapor deposition using a commercial evaporator (Focus, EFM 3, flux calibrated by a quartz microbalance) while keeping the sample temperature at 115 K. During metal evaporation, the sample was biased to avoid formation of defects by metal ions. The Pd coverage used to prepare the particles was 2.7×10^{15} atoms cm⁻². The particles were subsequently annealed to 600 K and stabilized by repeated cycles of oxygen (8×10^{-7} mbar for 1000 s) and CO (8×10^{-7} mbar for 3000 s) exposure at 500 K before use.¹⁴ According to the STM data,¹⁴ the surface displays Pd particles with an average diameter of 7 nm containing approximately 3000 atoms each. The particles uniformly cover the support with an island density of about 8.3×10^{11} islands cm⁻². The majority of the particles are well-shaped crystallites grown in the (111) orientation and terminated predominantly by (111) facets (~80%) as well as by a small fraction of (100) facets (~20%).

Before each experiment, the Pd/Fe₃O₄ model catalyst was cleaned by oxidation–reduction cycles as employed during stabilization of the Pd particles. For carbon precovering, the sample was exposed to 280 L of D₂ and 0.8 L of *cis*-2-butene at 100 K and heated in vacuum to 500 K in the following (see ref 15 for details).

AUTHOR INFORMATION

Corresponding Author

*E-mail: schauermann@fhi-berlin.mpg.de.

REFERENCES

- (1) van den Berg, A. W. C.; Arean, C. O. *Chem. Commun.* **2008**, 668.
- (2) Raimondi, F.; Scherer, G. G.; Kötze, R.; Wokaun, A. *Angew. Chem., Int. Ed.* **2005**, *44*, 2190. Huang, Y.; Dass, R. I.; Xing, Z.; Goodenough, J. B. *Science* **2006**, *135*, 757.

- (3) Daley, S. P.; Utz, A. L.; Trautman, T. R.; Ceyer, S. T. *J. Am. Chem. Soc.* **1994**, *116*, 6001.
- (4) Doyle, A. M.; Shaikhutdinov, Sh.K.; Jackson, S. D.; Freund, H.-J. *Angew. Chem., Int. Ed.* **2003**, *42*, 5240.
- (5) Teschner, D.; Borsodi, J.; Wootsch, A.; Révay, Z.; Hävecker, M.; Knop-Gericke, A.; Jackson, S. D.; Schlögl, R. *Science* **2008**, *320*, 86.
- (6) Wilde, M.; Fukutani, K.; Ludwig, W.; Brandt, B.; Fischer, J.-H.; Schauermann, S.; Freund, H.-J. *Angew. Chem., Int. Ed.* **2008**, *47*, 9289.
- (7) Ludwig, W.; Savara, A.; Schauermann, S.; Freund, H.-J. *Chem. Phys. Chem.* **2010**, *11*, 2319.
- (8) Webb, G. In *Comprehensive Chemical Kinetics*; Bamford, C. H., Tipper, C. F. H., Eds.; Elsevier: Amsterdam, 1978; Vol. 20, p 1. Bond, G. C., *Metal-Catalysed Reactions of Hydrocarbons*; Springer: New York, 2005.
- (9) Alefeld, G.; Völkl, J. *Hydrogen in Metals*; Springer: New York, 1978.
- (10) Fromm, E.; Gebhardt, E. *Gase und Kohlenstoff in Metallen*; Springer: New York, 1976.
- (11) Christmann, K. *Surf. Sci. Rep.* **1988**, *9*, 1.
- (12) Jewell, L. L.; Davis, B. H. *Appl. Catal. A: Gen.* **2006**, *310*, 1. Greeley, J.; Mavrikakis, M. *J. Phys. Chem. B* **2005**, *109*, 3460.
- (13) Neyman, K. M.; Schauermann, S. *Angew. Chem., Int. Ed.* **2010**, *49*, 4743.
- (14) Schalow, T.; Brandt, B.; Starr, D. E.; Laurin, M.; Schauermann, S.; Shaikhutdinov, S. K.; Libuda, J.; Freund, H.-J. *Catal. Lett.* **2006**, *107*, 189.
- (15) Brandt, B.; Fischer, J.-H.; Ludwig, W.; Libuda, J.; Zaera, F.; Schauermann, S.; Freund, H.-J. *J. Phys. Chem. C* **2008**, *112*, 11408.
- (16) Wilde, M.; Fukutani, K.; Naschitzki, M.; Freund, H.-J. *Phys. Rev. B* **2008**, *77*, 113412.
- (17) Conrad, H.; Ertl, G.; Latta, E. E. *Surf. Sci.* **1974**, *41*, 435.
- (18) Estimated from the TPD data using Redhead analysis and pre-exponential factor 10^{13} .
- (19) This condition applies if the isotope kinetic effects are neglected.
- (20) Gdowski, G. E.; Felner, T. E.; Stulen, R. H. *Surf. Sci.* **1987**, *181*, L147.
- (21) Okuyama, H.; Siga, W.; Takagi, N.; Nishijima, M.; Aruga, T. *Surf. Sci.* **1998**, *401*, 344.
- (22) Manchester, F. D.; San-Martin, A.; Pitre, J. M. *J. Phase Equilib.* **1994**, *15*, 62.
- (23) Flanagan, T. B.; Oates, W. A. *Annu. Rev. Mater. Sci.* **1991**, *21*, 269.
- (24) Libuda, J.; Meusel, I.; Hartmann, J.; Freund, H.-J. *Rev. Sci. Instrum.* **2000**, *71*, 4395.
- (25) Schalow, T.; Brandt, B.; Laurin, M.; Schauermann, S.; Libuda, J.; Freund, H.-J. *J. Catal.* **2006**, *242*, 58.